

Supplementary Materials for **Cellular uptake and dynamics of unlabeled freestanding silicon nanowires**

John F. Zimmerman, Ramya Parameswaran, Graeme Murray, Yucui Wang, Michael Burke, Bozhi Tian

Published 16 December 2016, *Sci. Adv.* **2**, e1601039 (2016)

DOI: 10.1126/sciadv.1601039

The PDF file includes:

- Supplementary Text
- table S1. Summary of inhibitor action on SiNW internalization.
- fig. S1. Perinuclear SiNW clustering.
- fig. S2. SiNW tracking algorithm.
- fig. S3. Stage drift controls.
- fig. S4. Linear SiNW transport trajectories.
- fig. S5. Migration coupled active transport.
- fig. S6. Serum-free SiNW internalization.
- fig. S7. Example MSD calculation.
- fig. S8. Nocodazole-inhibited SiNW transport.
- fig. S9. Active tug-of-war SiNW transport.
- fig. S10. Lysosome tracking.
- fig. S11. SiNW-cell colocalization determination.
- fig. S12. Concentration-dependent metabolic activity assay.
- fig. S13. Cell line-specific SiNW-cell colocalization.
- fig. S14. Ensemble HUVEC control samples.
- fig. S15. Multiple internalization events.
- fig. S16. Chlorpromazine-positive control.
- fig. S17. High-concentration A5 study.
- fig. S18. Cytosolic SiNW protein sheath formation.
- fig. S19. Prestained A5 SiNWs.
- fig. S20. Lova inhibitor study.
- Legends for movies S1 to S4

Other Supplementary Material for this manuscript includes the following:
(available at advances.sciencemag.org/cgi/content/full/2/12/e1601039/DC1)

- movie S1 (.mov format). Single-cell SiNW active transport.
- movie S2 (.mov format). Bidirectional active tug-of-war SiNW transport.
- movie S3 (.mov format). Macrophage internalization of SiNWs.
- movie S4 (.mov format). SiNW membrane engulfment.

Supplementary Text

Confocal Fluorescent Microscopy

Cells were cultured until approximately 40-50% confluent. Prior to staining, cells were incubated with SiNW for 24 hrs and fixed with 4% paraformaldehyde in phosphate buffered saline solution (PBS) for 20 mins at room temperature. The cells were then stained with TRITC-phalloidin (Millipore, FAK100, excitation laser 532 nm) and anti- α tubulin Alexa Fluor 488 (ThermoFisher 322588, Excitation laser 488 nm) following the manufactures' protocol. A Leica SP5 confocal microscope was used with an oil immersion objective (Leica 63x). SiNW scattering was monitored in a separate channel, using a 458 nm excitation laser, with scattered light detected at a similar wavelength, between 454-468 nm. At this wavelength, the scattering intensity from SiNWs was much greater than the underlying cells, and wires were readily distinguished using simple image intensity thresholding in NIH ImageJ.

Scanning Electron Microscopy Sample Preparation

SiNWs were sonicated into M200 growth media and transferred to a Petri dish containing a glass coverslip which had previously been sterilized using ethanol (30 second wash in 70% EtOH). SiNWs were allowed ~16 hrs to settle, before the media was removed and trypsinized HUVECs were introduced. After ~18 hrs of incubation, samples were fixed using 4% paraformaldehyde in a phosphate buffered saline (PBS) solution. Samples were then washed twice using fresh PBS and dehydrated using subsequent ethanol substitution steps (20%, 40%, 60%, 80%, 90%, 95%, 100% x2, 15 min each). Next, samples were dried using a CO₂ critical point dryer (Leica EM CPD300 Critical Point Dryer), and a 6 nm Pt/Pd layer was deposited onto the fixed cells using a sputter coater (Ted Pella). The glass substrate was then mounted using conductive carbon tabs and imaged using a FEI Nova NanoSEM 230. For transmission electron microscopy studies, samples were prepared and processed as previously reported (27).

Single Nanowire Transport

Individual SiNWs were tracked using Scattered Enhanced Phase Contrast (SEPC) imaging. To prepare samples, SiNWs were first rinsed with hydrofluoric acid (HF, Sigma Aldrich)(9.8%) for 10-30 seconds, before being washed in DI water. To sterilize the SiNWs, they were then transferred to a 70% ethanol solution, and kept under an ultraviolet lamp for ~30 mins. Next, the SiNW substrate was then transferred to the appropriate cell media and sonicated for 7 mins to suspend the SiNWs into solution. The media containing the SiNWs was then transferred to a glass-bottom petri dish, and allowed to settle for ~16 hrs. During this period, media was stored in a cell incubator at 37° C and 5% CO₂. Next, the media was aspirated, cells were seeded onto the petri dish (Note that samples were not fully dried during aspiration, as this was observed to reduce SiNW uptake in some cases). Cells were then given ~20 mins to attach to the petri dish before being transferred to a stage top incubator (INUB-ONICS-F1 Takai Hit) which maintained physiological conditions (i.e. 95% humidity, 37°C internal temperatures, 5% CO₂) during sample imaging. Internalization was then monitored using SEPC, where images were recorded on a Hamamatsu ORCA-R2 C10600-10B digital CCD camera at 16bit depth with pixel resolutions between 0.3 μm x 0.3 μm to 0.1 μm x 0.1 μm, depending on the objective used.

To resolve the SiNW's position, SEPC images were first thresholded using NIH ImageJ, yielding binary images of just the SiNW (fig. S2). In some cases images were preprocessed and backgrounds were subtracted using a Gaussian spatial filter uniformly applied to each image. The SiNW's profile was approximated as linear and was fit on a per frame basis using a linear least squares regression in python, returning the position of each nanowire tip. For SiNW profiles with slopes greater than 45°, the profiles were rotated 90° to preserve them as a function, before fitting. The resulting tip positions were then rotated back into the original coordinate system. All SiNW trajectories were corrected for stage drift by also recording the "motion" of stationary particles external to the SiNW-Cell system (fig. S3), which was fit using a similar process. Instantaneous velocities were determined on a rolling frame basis, by averaging the distance travelled by particles over a 15 frame interval, to smooth sample noise. Mean squared displacements (MSD) were determined by calculating the distance

that an individual NW was displaced after a given lag time averaged for an entire trajectory. In this case trajectories were segmented into rolling intervals (typically between 30-60 frames depending on the sampling rate), centered on the reported time point. Values for α were obtained by fitting the Ln-Ln plot of the MSD with a linear regression (fig. S7), with the slope yielding the relative diffusivity exponent α . Slopes with negative values of the Ln-Ln plot were observed for the stationary case, and were approximated as being zero.

MTT Assay and SiNW Counts

Four different sized wafers containing 100 nm SiNW were etched in 9.8% HF for 20 seconds. Samples were then washed with DI water and dried under N₂ gas. They were then immersed in 70% ethanol for 30 min under UV light and sonicated into 8 mL of M200 media for 7 mins. Plating the nanowires for the MTT assay, 50 μ L of media containing SiNWs were then aliquoted into a 96 well plate, with eight replicates of each nanowire concentration condition and a set of "blank" (i.e. no NWs) wells. Additionally, to assist with SiNW counting, a 10 μ L droplet of each SiNW mixture was placed onto a glass slide and was capped using a glass coverslip of a known area such that the media formed a continuous coverage under the coverslip. For each nanowire mixture, 8 images of were taken in darkfield at predetermined locations and nanowires were subsequently counted using NIH's imageJ. Using the known coverslip area, and total droplet volume, the SiNW concentration was back calculated. After allowing the SiNWs to settle overnight in the 96 well plate, the 50 μ L of media left over was replaced with 50 μ L of HUVEC cells at ~30% confluency. Cells were then incubated with the nanowires for 3 days, changing media at the 24 hrs mark. Additional control samples containing no SiNWs were also plated. Next, 20 μ L of MTT was added to the cells at a concentration of 5 mg/mL and left to incubate at 37° C for 3 hrs. The media and MTT were then replaced with 100 μ L of dimethyl sulfoxide (DMSO) and the sample was left to incubate on a shaker for 15 mins in the dark at room temperature. Colorimetric measurements were then taken on a spectrophotometer plate reader at 570 nm and 660 nm (reference) wavelengths.

Ensemble Lysosome Overlap

SiNWs were first sonicated (~10 min) into M200 media and transferred to a glass-bottom petri dish, where the SiNWs were allowed to settle overnight. Prior to co-incubation, HUVECs were pre-stained with LysoTracker Blue for 2 hours (DND-22, ThermoFisher Scientific), following the manufacturer's protocol. Next, cells containing the lysotracker were trypsinized and transferred to the petri dishes containing SiNWs. Colocalization was monitored at 1, 2 and 3 hours respectively in the darkfield, phase contrast, and DAPI fluorescent channels (Olympus IX71 inverted scope) (fig. S10). For each time point, a series of images were taken at predetermined locations prior to viewing to prevent observational bias. Micrographs were then processed using NIH imageJ, with SiNWs showing at least a segment of the wire as colocalized with a lysosome (fig. S10A, a) being counted as "overlapping", as compared to those wires which also showed cellular overlap, but no colocalization with lysosomes (fig. S10A, b).

Neonatal Rat Ventricular Cardiomyocytes Isolation

Hearts were excised from decapitated P2 neonatal Sprague-Dawley rats and placed into HBSS without Ca^{2+} or Mg^{2+} on ice. Hearts were washed in HBSS on ice six times to eliminate as many red blood cells as possible. Atria were sliced off of the hearts over ice, and each heart was minced into 3-4 pieces and transferred into 0.05 mg/mL trypsin in HBSS. Hearts were incubated overnight in trypsin on a 4°C cold room shaker. Hearts were then transferred to a 37°C water bath. 2 mg/mL soybean trypsin inhibitor in HBSS was added to the hearts followed by 1 mg/mL collagenase type II in L15 medium. Hearts were incubated in the water bath with collagenase for 45 mins, with manual shaking and inverting every 5 min. Slow mechanical trituration of the cells was then performed in the tissue culture hood ten times with a plastic pipette. Next, cells were passed through a 70 µm filter and allowed to rest for 30 mins at room temperature. Cells were then centrifuged and resuspended into DMEM + 10% FBS + 100 U/mL penicillin + 100 µg/mL streptomycin cardiac culture medium. Cells were plated on 10 cm TC treated petri dishes in a 37°C 5% CO_2 cell culture incubator for 2 hrs in order to adhere the smooth muscle and fibroblast cells to the plastic and exclude them from the cardiac culture. After the incubation, the cardiac cells in the supernatant were counted via

trypan blue staining. Cardiac cells were plated on glass bottom petri dishes coated with fibronectin and pre-settled SiNWs at a concentration of 5×10^5 cells/dish. All rats were used in accordance with the University of Chicago's Animal Care and Use Protocol (ACUP: 72378) and the National Institutes of Health guidelines.

Dorsal Root Ganglia Culture

Dorsal root ganglia were dissected from decapitated P1 neonatal Sprague-Dawley rats into DMEM on ice. Ganglia were resuspended into 2.5 mg/mL trypsin in EBSS for digestion in a 37°C shaker for 20 mins. Following the digestion, cells were spun down and resuspended into 10% FBS in EBSS to inhibit any remaining trypsin. Mechanical trituration of the cells was then performed using three glass pipettes of decreasing size. Cells were centrifuged and resuspended into culture media consisting of DMEM + 5% FBS + 100 U/mL penicillin + 100 µg/mL streptomycin. They were then seeded onto the Poly-L-lysine coated glass bottom dishes with pre-settled SiNWs and left in a 37°C 5% CO₂ cell culture incubator for 25 mins to adhere to the glass. After the adhesion incubation, dishes were flooded with the same media until further use. Glass bottom dishes were prepared by soaking in Poly-L-lysine for ~25 mins, before being rinsed twice in PBS. SiNWs were then sonicated into DMEM + 5% FBS, and allowed to settle ~18 hrs before being used for cell culture. All rats were used in accordance with the University of Chicago's Animal Care and Use Protocol (ACUP: 72378) and the National Institutes of Health guidelines.

Nocodazole Inhibitor

Silicon wafers containing 100 nm SiNWs were first etched in 10% HF for 20 seconds, and were then washed with DI water and dried under N₂ gas. Samples were then sterilized in 70% ethanol for 30 min under UV light, before being sonicated into 10 mL of M200 HUVEC cell media for 7 mins. Next, 1 mL of the resulting SiNW mixture was aliquoted into a 35 mm petri dish and allowed to settle overnight. Media was then aspirated and HUVEC cells were introduced at ~30% confluence in M200 media containing 60 µM nocodazole (Sigma 487928). Cells were allowed 15 mins to attach to the substrate in a 37° C incubator, before being transferred to a stage top

microincubator (INUB-ONICS-F1 Takai Hit) for imaging. Videos were taken of cellular SiNW uptake for 1-2 hrs using SEPC, and analyzed as described above for other single SiNW dynamics experiments.

Chlorpromazine Positive Control Drug Studies

To confirm that clathrin was successfully inhibited at these drug concentrations, Texas Red conjugated transferrin (from human serum, Life Technologies) was used as a positive control. HUVECs were transferred to fresh glass substrates via trypsinization and allowed to incubate for 8 hrs. For the inhibitor samples, 6.45 μL of chlorpromazine (3.1 mg/mL) dissolved in DMSO was added to 8 mL of M200 growth media, which was then distributed to the HUVEC growth culture for 30 minutes, before adding conjugated transferrin dissolved in deionized water for a final working concentration of 25 $\mu\text{g/mL}$. For the control samples, a similar process was followed, using blank DMSO containing no chlorpromazine. Both samples were then allowed to incubate for 14 hrs, before being washed twice in 1x PBS, and then fixed using 4% paraformaldehyde (20 mins). The samples were then rinsed twice more in fresh PBS and imaged at random locations (determined prior to viewing to prevent sample bias) using the same exposure and intensity settings on an Olympus IX71 inverted microscope under a Texas Red filter. The mean fluorescent intensity of each image was then obtained using NIH's ImageJ, and normalized by cell count.

SiNW Optical Scattering in Protein Corona Formation

SiNWs optical scattering was determined as previously reported (1). Briefly describing this process, first SiNWs (100 nm diameter) were sonicated into deionized water and into M200 media respectively. For cell samples, cells were first trypsinized and then transferred to a fresh petri dish using the media containing the SiNWs. Both water controls and cell samples were then kept under physiological conditions for the duration of the experiment (37°C, 5% CO₂). As SiNWs take some time to settle, optical profiles were first measured 25 hours after incubation, with profiles measured at 48, 72, and 96 hours respectively. To measure SiNW scattering intensity, optical profiles were taken transverse to the SiNWs at an angle of 90° (fig. S18B), with illumination intensity and image exposure times maintained across all samples. Background noise was then

subtracted using a linear deconvolution fit to the profile base, and cell sample scattering intensities were normalized as compared to the control deionized water scattering. We note here that no significant deviation was observed in the deionized water control sample's scattering intensity over the duration of the experiment.

A5-Cy3 Surface Functionalization

Wafers containing SiNWs were first plasma cleaned (200w Plasma Etch 100LF) for 1 min at 100 W. Under a nitrogen atmosphere, chips were then immersed in a 1% v/v 3-(trimethoxysilyl)propylaldehyde in ethanol/H₂O(95%/5%) solution for 30 minutes, before being rinsed with an ethanol flow, and dried using hot N₂ gas (110° C) for 10 minutes. Still under nitrogen, chips were then immersed in an A5-Cy3 containing buffer solution (10–100 µg/ml A5-Cy3, 10 mM PBS, pH 8.4, 4 mM sodium cyanoborohydride) for 3h. The sample was then rinsed using a 10 mM PBS (pH 8.4), and unreacted aldehyde surface groups were passivated by soaking the chip in 100 mM ethanolamine in 10 mM phosphate buffer, pH 8.4 in the presence of 4 mM cyanoborohydride for 2 hrs. Samples were then rinsed once more with 10 mM PBS (pH 8.4), before being sonicated (2 min) into solutions for experimental use. After 24 hrs of co-incubation with cells (37° C, 5% CO₂), samples were then fixed using 4% paraformaldehyde for 20 mins, and imaged under the same optical conditions (i.e. exposure, light intensity, etc). This functionalization process gave a 54±15% yield of SiNWs which showed appreciable fluorescence signal after treatment (determined for wires incubated in PBS at 37° C, 5% CO₂, in the absence of cells). This portion of unmodified wires acts as a useful internal standard, and was used to study the distribution of modified versus unmodified wires during internalization.

2D Random Walker Model

While monitoring ensemble rates of SiNW internalization, we observed a pattern of nanowire internalization where SiNWs remain stationary on the substrate, while cells migrate across the surface picking up nanowires. This mode of internalization is distinct from normal routes of drug delivery, where the cells are stationary and drugs are mixed ubiquitously into a solution. As a result, this internalization process would be expected

to follow a distinct model of kinetics, differing drastically from other drug delivery mechanisms.

The present case of NW internalization can be considered in terms of a two dimensional (2D) random walk model, where cells are diffusive walkers that crawl over the surface of a lattice, with equal probability of moving in any direction. As a cell visits a new lattice site, this area has the chance of containing a nanowire (assuming a uniform nanowire surface coverage), which the cell can then internalize. Once internalized, a NW will remain with the cell as it moves to new lattice sites, marking the previous site as having been visited. In this case, the percentage of NWs internalized should be proportional to the total number of sites visited by all of the cells inside of the system. What follows is a model for the number of unique sites visited by an ensemble of random walkers, which we show is in good agreement with experimental data for nanowire internalization.

Variable Definitions

N = Total number of walkers

A_{total} = Total number of lattice sites

n = Number density of walkers (N / A_{total})

τ = Number of steps

$A_1(\tau)$ = Expected number of distinct sites that have been visited by **an individual** walker after τ steps

$A_N(\tau)$ = Expected number of distinct sites that have been visited by **all** walker after τ steps

$Pr(\tau)$ = Probability that an individual site has **not** been visited after τ steps

$Y(\tau)$ = Probability that an individual site **has** been visited after τ steps

The number of nanowires internalized should be proportional to the total number of distinct sites visited by all of the random walker as a function of steps or time ($A_N(\tau)$). The percentage of nanowires internalized should be equal to this value divided by the total area ($A_N(\tau) / A_{total}$), where A_{total} is the total number of lattice sites. A direct solution for $A_N(\tau)$ is not available but we can use the following formulation.

The probability that a site has not been visited by one specific random walker at step i can be taken to be

$$\Pr(\tau)_i = 1 - \frac{A_1(\tau)}{A_{total}} \quad (\text{S1})$$

Therefore, if there are N number of walkers it follows that

$$\Pr(\tau)_N = \prod_{i=1}^N \Pr(\tau)_i = \left(1 - \frac{A_1(\tau)}{A_{total}}\right)^N \quad (\text{S2})$$

N can also be defined in terms of walker density, such that $N = n \cdot A_{total}$, such that

$$\Pr(\tau)_N = \left(1 - \frac{A_1(\tau)}{A_{total}}\right)^{n \cdot A_{total}} = \left(1 - \frac{n \cdot A_1(\tau)}{n \cdot A_{total}}\right)^{n \cdot A_{total}} \quad (\text{S3})$$

Using the property of Euler's number, e , such that

$$\lim_{n \rightarrow \infty} \left(1 + \frac{x}{n}\right)^n = e^x \quad (\text{S4})$$

it can be shown that for a large number of lattice sites, such that $A_{total} \rightarrow \infty$, then the probability that an individual site has not been visited by any random walker after τ steps is given by

$$\Pr(\tau)_N = e^{-n \cdot A_1(\tau)} \quad (\text{S5})$$

This value while useful, is dependent on the nebulous term $A_1(\tau)$, the expected number of distinct sites that have been visited by a single 2D random walker after τ steps. A rigorous determination of this function is beyond the scope of this manuscript, however in 1951 Dvoretzky & Erdős (41) demonstrated that in a 2D system this follows the form of

$$A_1(\tau) = \frac{\pi\tau}{\log \tau} + B_0 \quad (\text{S6})$$

where B_o is a higher order correction term, where we have approximated $n \cdot B_o$ as constant over the duration of the experiment. As the probability that a given site will have been visited, $Y(\tau)$, is defined by the function $Y(\tau) = 1 - \Pr(\tau)_N$, it follows that

$$Y(\tau) = 1 - e^{\frac{-n\pi\tau}{\log\tau} \cdot n \cdot B_o} \quad (\text{S7})$$

However, this formulation assumes that each nanowire once contacted by a walker is available for internalization, an assumption which may prove improbable due to morphological restrictions or limitations in surface functionalization of the NWs. Therefore, this result is better expressed as

$$Y(\tau) = M_w - e^{\frac{-n\pi\tau}{\log\tau} \cdot n \cdot B_o} \quad (\text{S8})$$

where M_w is the maximum percentage of NWs available for internalization. In practice, M_w is found to have values of ~ 0.96 in HUVECs, suggesting that it's substitution is not completely unwarranted, however this distinction could prove useful when looking at future nanoconstructs which have less ubiquitous rates of internalization.

This function than gives us the probability for a NW to internalized, which should be reflected in the percentage of nanowires that will have been internalized after τ steps, however this function only holds in the discreet site limit and over a large number of step. Therefore to use this in a real world situation, it becomes desirable to take this into the continuum limit. While a rigorous expansion to the continuum case is beyond the scope of this manuscript, some features of the continuum model are readily apparent. For example, τ must be proportionate to time, t , such that $\tau \sim D_t \cdot t / A_{cell}$, where D_t is a diffusion constant relating the amount of time it takes to move across the lattice and A_{cell} is the average area of an individual cell, relating the size of the walker to the size of the lattice. Similarly, the value of $\log \tau$, is a good approximation only in the long term limit, and is therefore inappropriate for modeling real world experiments, as cells have a relatively slow migration rate. Finally, the density of random walkers does not remain constant over the duration of the experiment, as cells are able to undergo mitosis,

therefore the number density of walkers in a continuum case is more appropriately measured as function of percent confluence, $C(t)$, (the percentage of the surface covered by cells). The percent confluence in the continuum model can be related to the number density in discrete model by $n = C(t)$. All of these factors taken into account result in continuum model equation of the form

$$Y(t) = M_w - B e^{-\frac{\pi D_t \cdot C(t) \cdot t}{A_{cell}}} \quad (\text{S9})$$

where the rate constant, D_t , can be used as the single free fitting parameter. This yields an approximate expression for the rate of NW internalization. However, there is an additional boundary condition to consider. At time zero we know that the expected overlap, $Y_{(0)}$, should be equal to initial confluence $C_{(0)}$. That is to say that the number of sites initially occupied by walkers is proportional to the initial number of walkers. Additionally, at $t=0$, the right side of eq. S9 collapses, giving the expression

$$Y_{(0)} = C_{(0)} = M_w - B \quad (\text{S10})$$

which upon rearrangement yields, $B = M_w - C_{(0)}$. This allows B , which was initially conceived of as higher order correction term, to be expressed in terms of the experimentally determined constants M_w and $C_{(0)}$. For simplicity we leave the expression for NW internalization in the form of eq. S9, however noting that the correction term, B , can be substituted for experimentally determined values.

Supplementary Table and Figures

table S1. Summary of inhibitor action on SiNW internalization.

Condition	Inhibits	χ^2	P
Control (No Drug)	--	1.6	0.95
Chlorpromazine	Clathrin	1.8	0.94
Nystatin	Lipid Rafts	1.7	0.97
Cytochalasin D (Positive Control)	Actin Polymerization	35.3	<<0.01
Dynasore	Dynamain	23.5	<<0.01
Annexin V (16 nM)	Phagocytosis	8.4	0.14
Lovastatin	Cholesterol	16.2	0.04

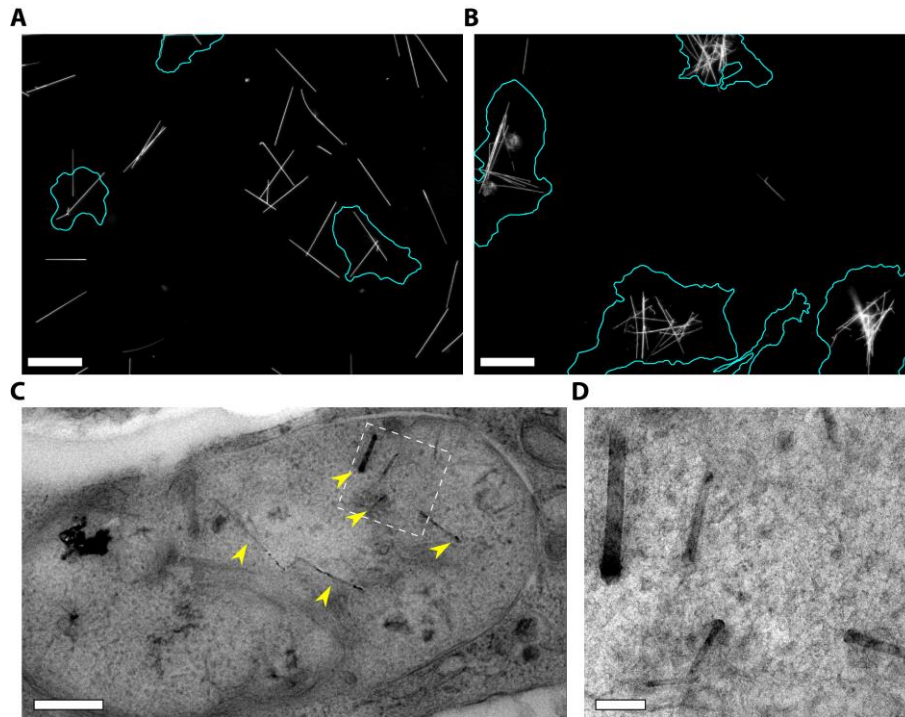


fig. S1. Perinuclear SiNW clustering. (A and B) Darkfield micrograph of SiNWs with HUVECs after 3 hrs and 48 hrs of incubation respectively, showing that SiNWs cluster with the cells over time. Highlighted teal regions indicate cell borders as determined by phase contrast microscopy (Scale Bars 50 μm). (C) Single large lysosomal type vesicle containing multiple SiNWs, with corresponding (D) higher magnification micrograph of the indicated region. Yellow arrows indicating the location of example SiNWs (Scale bars: 750 nm & 150 nm, respectively).

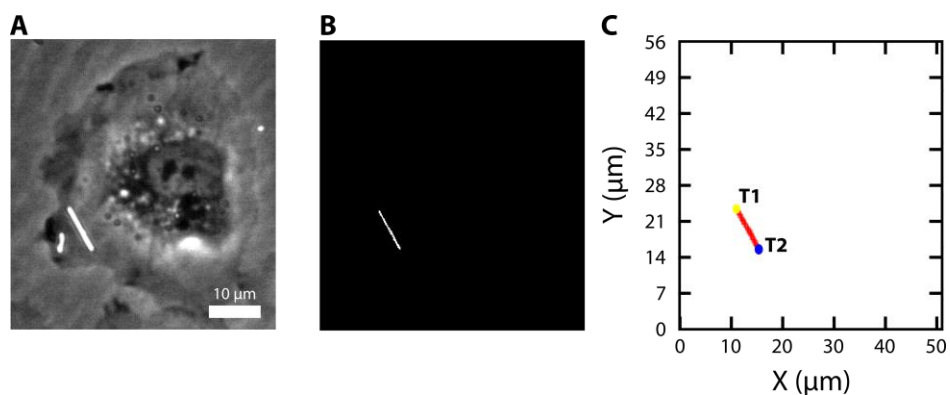


fig. S2. SiNW tracking algorithm. (A) Example SEPC micrograph of a SiNW mid internalization. (B) An intensity threshold filter is applied to the SEPC micrograph, and turned into a binary image containing only the SiNW of interest. SiNW coordinates are extracted using NIH imageJ, and (C) fit using a linear regression in python to return the position of internalized tip 1 (T1, yellow) and internalized tip 2 (T2, blue).

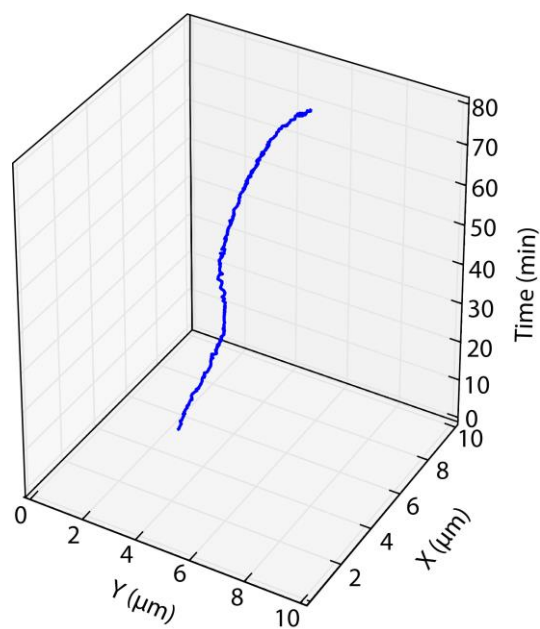


fig. S3. Stage drift controls. Example path of a 'stationary particle', indicating the amount of stage drift for a SiNW tracking experiment. Relative movement was subtracted to accommodate for drift of the stage.

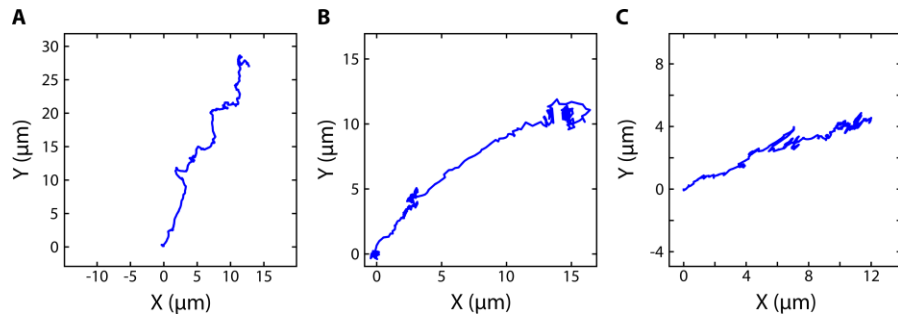


fig. S4. Linear SiNW transport trajectories. Example trajectories of three different SiNWs during intracellular transport, showing that many trajectories are relatively linear. Samples minorly smoothed using a less than 1% rolling average for clarity.

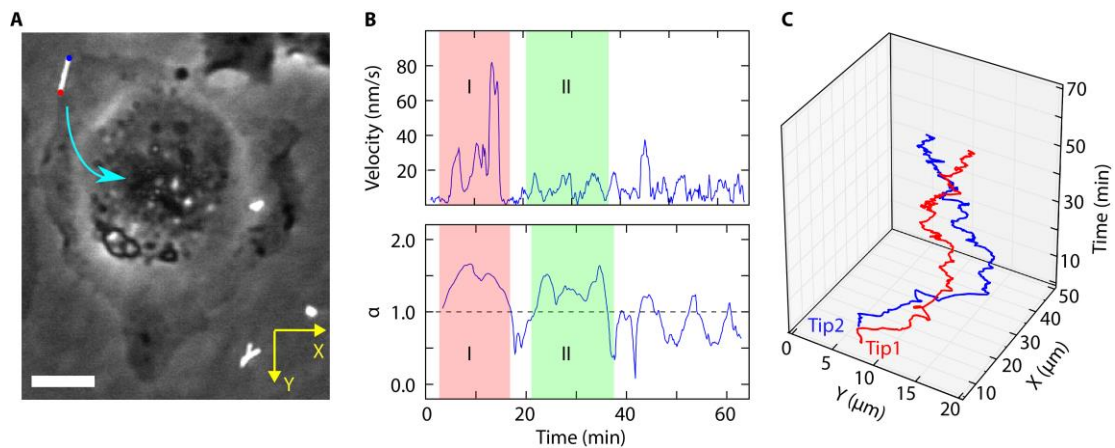


fig. S5. Migration coupled active transport. (A) SEPC micrograph of a SiNW being internalized by a HUVEC. (Scale bar 5 μm). SiNW tip 1 and 2 indicated by red and blue dots respectively, with the teal arrow indicating the general direction of SiNW travel. (B) Instantaneous velocity of the SiNW during active transport (15 frame average), with the corresponding rolling MSD 'diffusivity exponent', α , showing active transport process (Rolling 50 frame period). Highlighted regions indicate motor protein linked (I) active transport where SiNW tip velocity is greater than baseline, and cell motility (II) linked active transport where NW velocities are minor, but directional transport is given by the cell's general motility. All values given for tip 1 (red). (C) Path of travel for each tip of the SiNW as a function of time. SiNW rotation can be seen where the paths cross over one another.

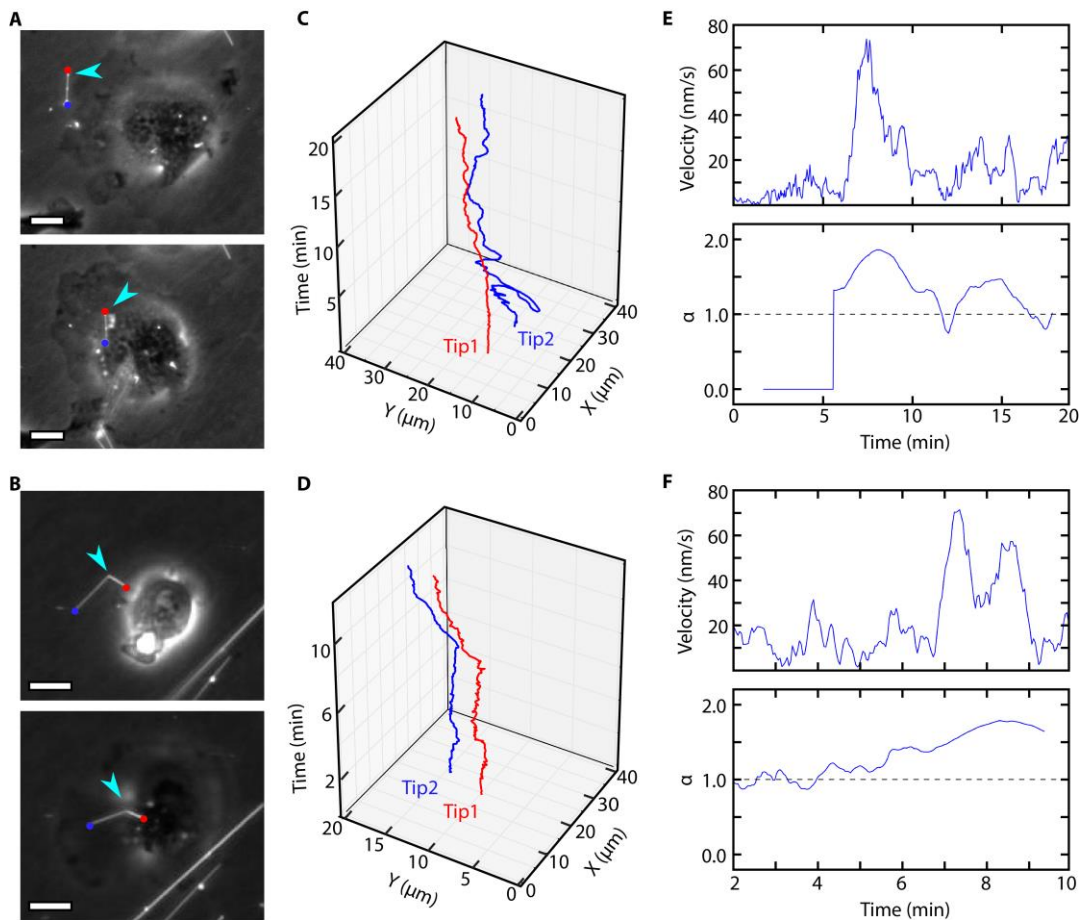


fig. S6. Serum-free SiNW internalization. (A and B) SEPC micrograph of a straight (A) and kinked (B) SiNW, before (upper) and after (lower) being internalized by a HUVEC in a serum free solution (10 μm scale bars). Teal arrow indicating the location of the tracked wire. Tip 1 indicated by red highlight (C and D) Path of travel of the SiNWs as a function of time for the straight and kinked SiNWs respectively. (E and F) Instantaneous velocity of the SiNW's tip during active transport (15 frame average), with the corresponding rolling MSD 'diffusivity exponent', α , showing that SiNWs can be internalized in the absence of opsonization (Rolling 55 frame period). (All values given for the highlighted red tips).

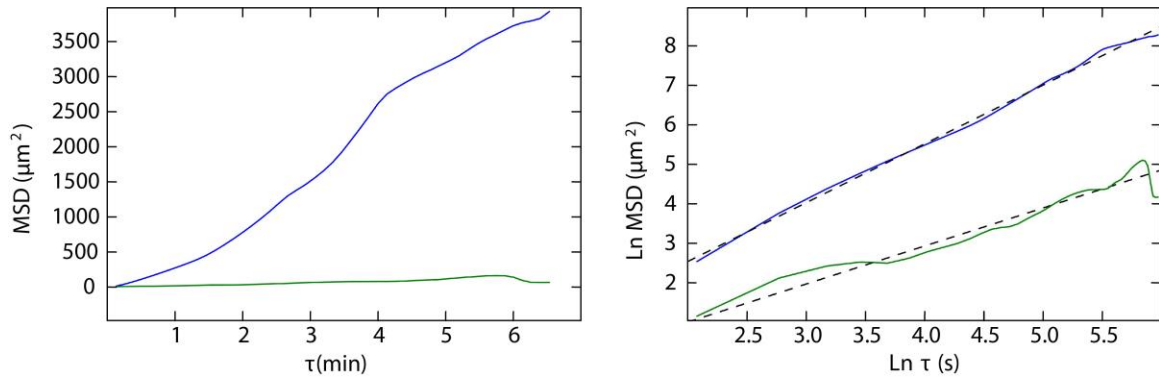


fig. S7. Example MSD calculation. The MSD of a SiNW that is being internalized at 13.5 min (blue) and 60 min (green) respectively, with corresponding Ln-Ln plot used to calculate the diffusivity exponent, α . Linear fits given as dashed line (Slopes: 1.49 & 0.96 respectively).

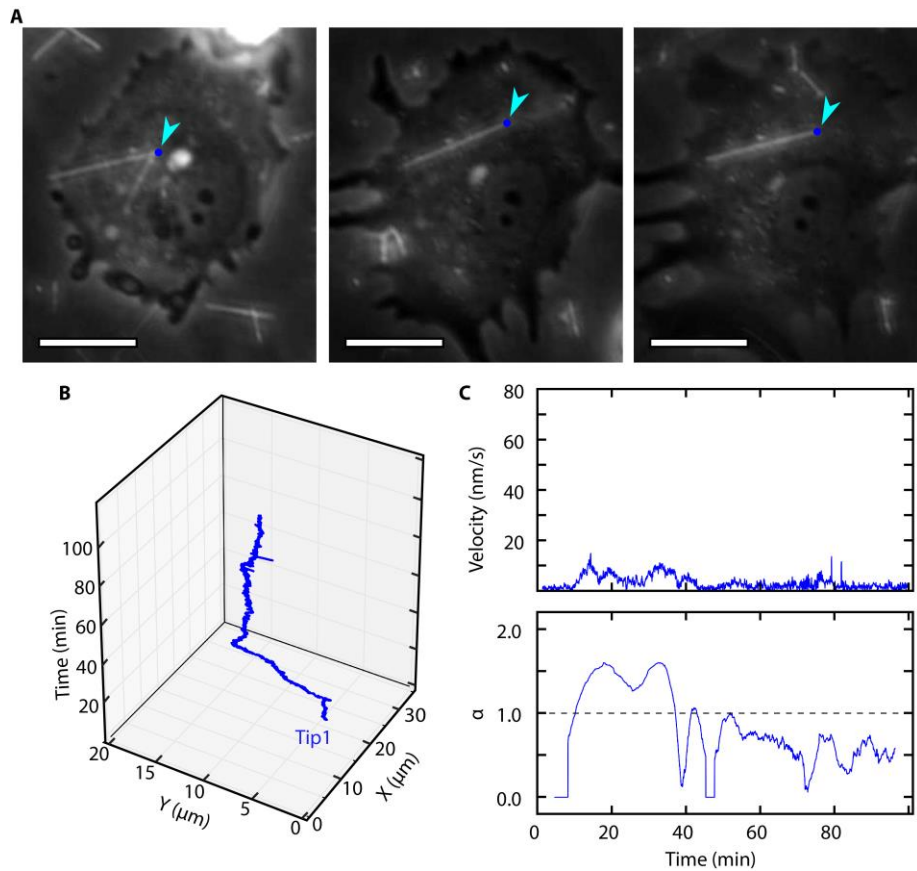


fig. S8. Nocodazole-inhibited SiNW transport. (A) SEPC micrographs of a SiNW being internalized after administering the microtubule inhibitor nocodazole, a microtubule inhibitor. (Time-lapse left to right: 0 min, ~50 min, ~100 min. Scale bar 20 μm). SiNW tip 1 indicated by the blue dot, and highlighted with the teal arrow. (B) Path of travel of the leading SiNW tip as a function of time. (C) Instantaneous velocity of the SiNW, with the corresponding rolling diffusivity exponent, α . Nocodazole treated cells showed minimal transport velocities, exhibiting active transport only during the initial, actin directed portion of internalization.

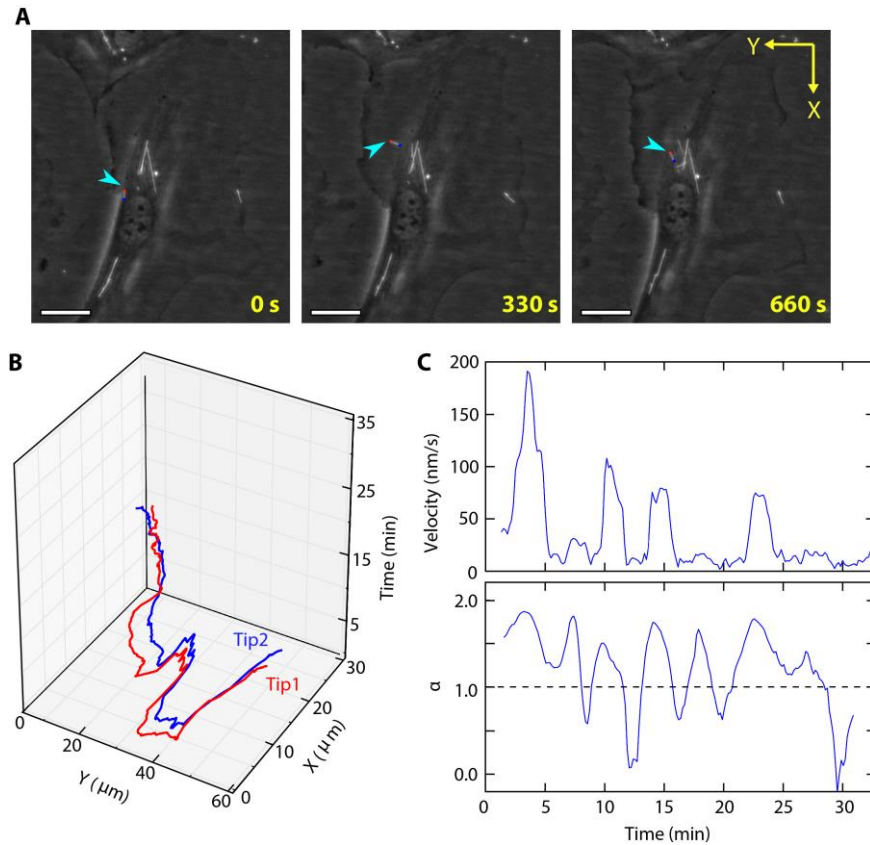


fig. S9. Active tug-of-war SiNW transport. (A) Timelapse SEPC micrographs of a SiNW after three days of co-incubation with a HASMC. (Scale bar 25 μm). SiNWs tips indicated by red and blue dots respectively, and the SiNW position highlighted by the teal arrow. (B) Path of travel the SiNW's tip as a function of time, showing a retraced "back and forth" motion. (C) Instantaneous velocity of the SiNW, with the corresponding rolling diffusivity exponent, α , showing large spikes in nanowire movement.

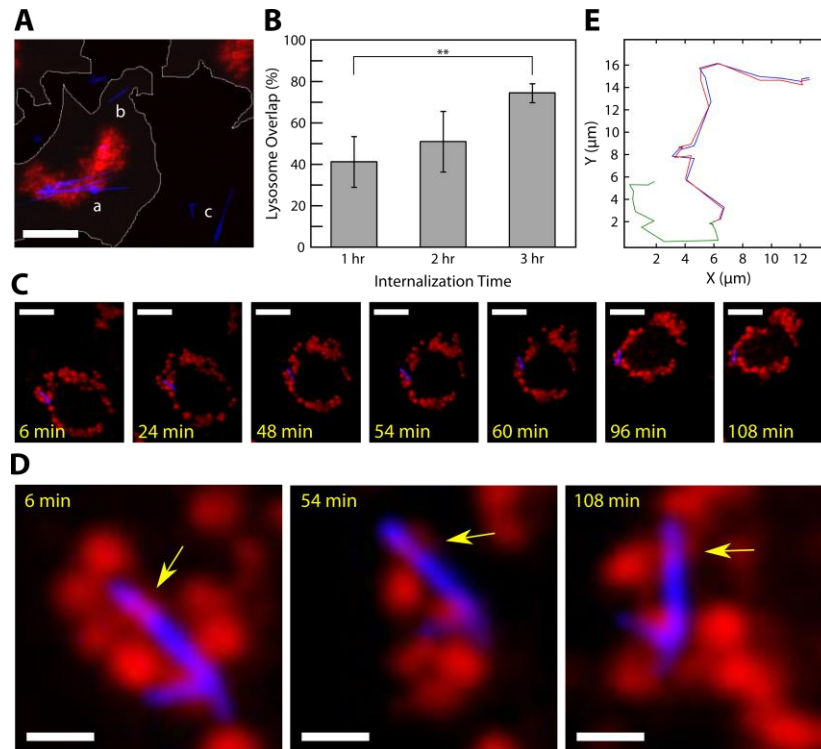


fig. S10. Lysosome tracking. (A) Example fluorescent micrograph after 3 hrs of incubation with HUVECs, used for determining ensemble lysosome overlap (red-Lyotracker, blue-DF scattering, white-cell outline), depicting SiNWs clustered with lysosomes (a), SiNW colocalized with the cell but not with any lysosomes (b), and (c) SiNWs outside of the cell. Scale bar 15 μm . (B) Ensemble percentage of SiNWs overlapping lysosomes as a function of incubation time. Percentage determined using only wires in contact with cells (populations a & b); excluding external wires (population c) as these have not yet been internalized (** indicates statistical significance, $P < 0.01$, $N = 9$). (C) Example time series of a single SiNW colocalized with a lysosome, with zoomed in inset at highlighted time points (Blue-scattering, red-Lyotracker Red) (D) showing that while SiNWs overlap with a large number of lysosomes, individual lysosomes can remain colocalized on the hour timescale (indicated by arrows). Scale bars are 8 μm (C) and 1.5 μm (D). (E) Trajectory of an individual lysosome (red), and the tip of a nearby SiNW (blue), as compared to a free particle in solution (green) (6 min/frame, total time = 108 min). SiNW movement is closely coupled to the lysosome, however both are driven by the underlying cell motility.

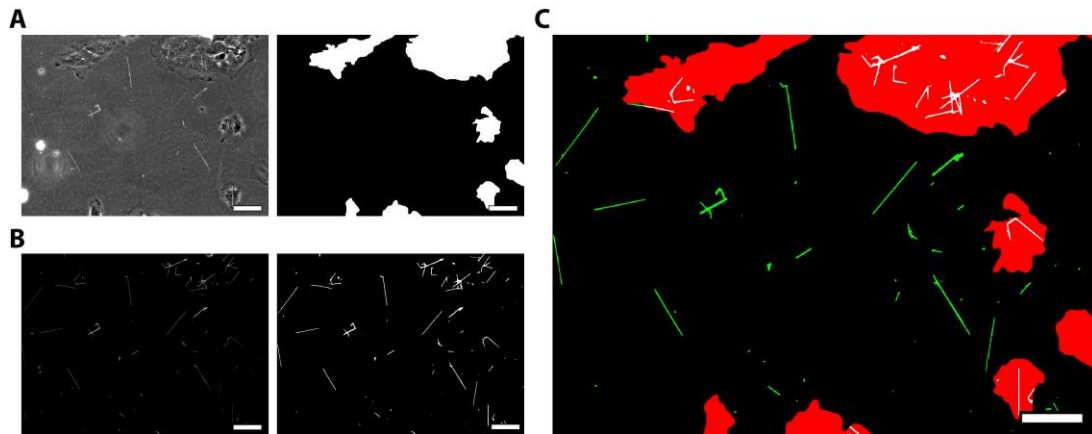


fig. S11. SiNW-cell colocalization determination. (A) Phase contrast micrograph of cells 4h after co-incubation (left), and the corresponding binary cell outline (right). (B) Darkfield micrograph with the same field of view, highlighting the SiNWs (left), and the corresponding binary image (right). (C) The resulting composite overlap image, depicting the cell's position (red), the overlapping SiNWs (white), and the excluded SiNWs (green). The percentage of SiNW-Cell overlap was determined on a per-pixel basis to incorporate wires which were only partially overlapping with cells. (all scale bars: 50 μm).

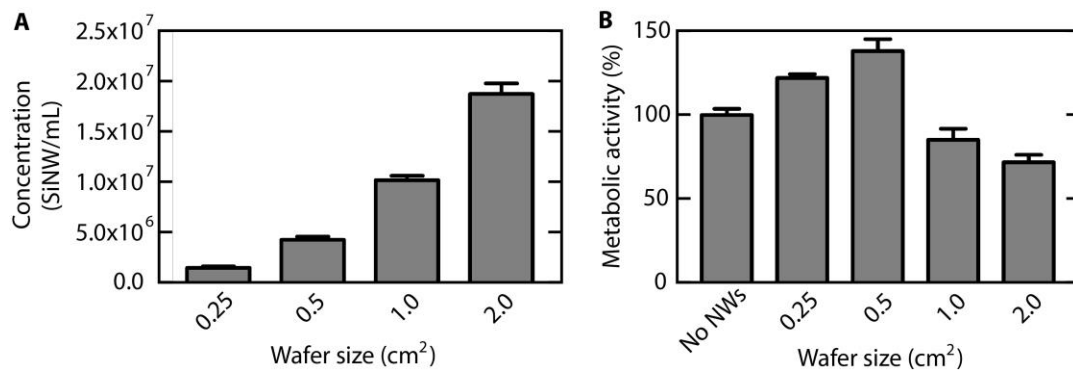


fig. S12. Concentration-dependent metabolic activity assay. (A) SiNW concentration was dependent on the size of the seeding wafer, with larger substrates providing more SiNWs. **(B)** MTT metabolic activity assay of HUVECs cultured with varying concentrations of SiNWs, showing increased metabolic activity at low concentrations, with mild cytotoxicity at higher concentrations. All values obtained on Day 3 of cell culture, and are presented relative to the SiNW free control. All error bars given as the standard error in measurement.

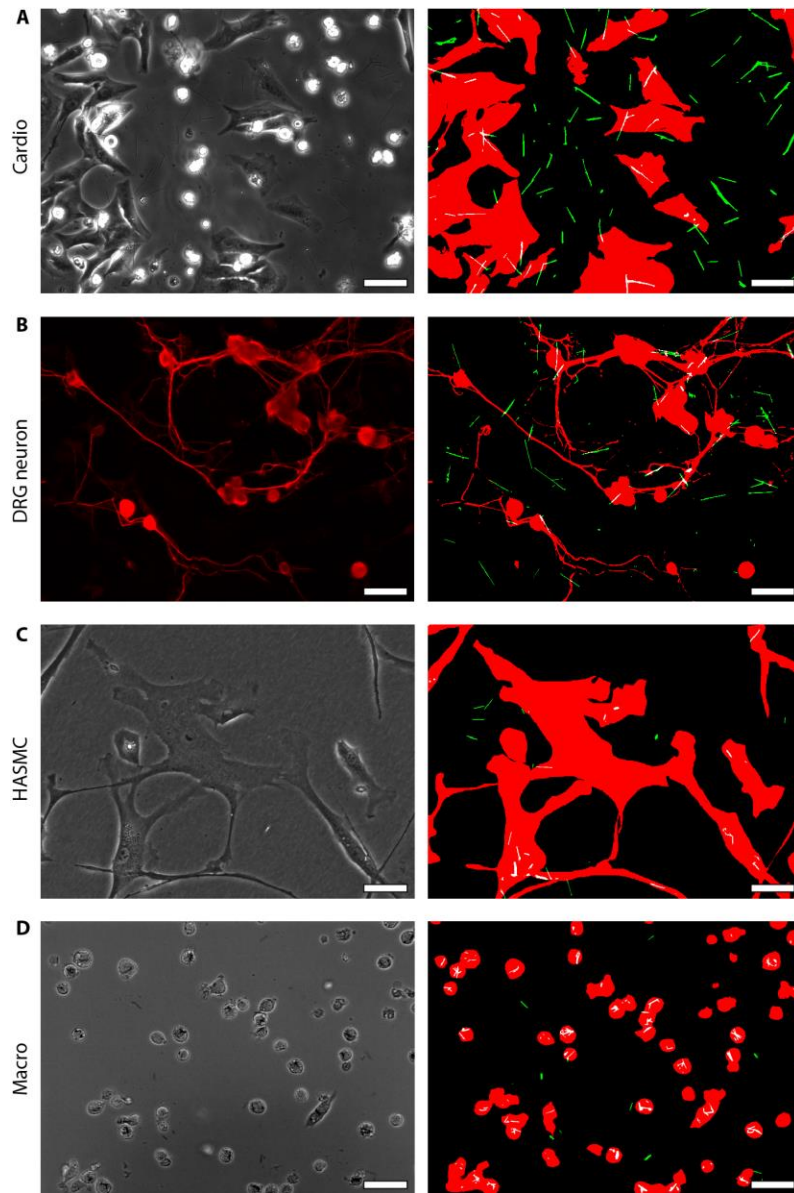


fig. S13. Cell line-specific SiNW-cell colocalization. Phase contrast micrograph of primary cardiomyocytes (Cardio) (A, left), Human Aortic Smooth Muscle Cells (HASMCs)(C, left) and J774A.1 macrophage cells (Macro) (D, left) and the TxRed channel of β -tubulin III stained DRG neurons (B, left), 24 hours after co-incubation with SiNWs, with the corresponding composite overlap image (A to D, right) depicting the cell's position (red), the overlapping SiNWs (white), and the excluded SiNWs (green) (all scale bars: 50 μ m).

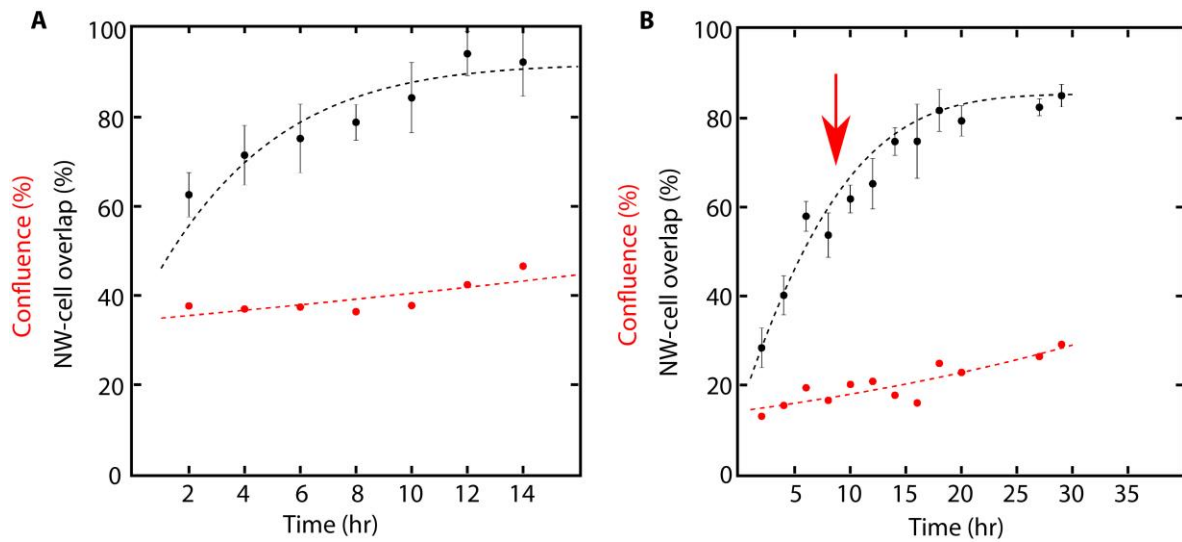


fig. S14. Ensemble HUVEC control samples. (A) Increased initial HUVECs concentration, showing cell confluence plays an important role in ensemble uptake dynamics. SiNW/Cell overlap (black dots) & cell confluence (red dots) as a function of time with modeled fit (black line). (B) Negative internal control of SiNW/Cell overlap, indicating the internal control model matched well with the resulting overlap in the absence of inhibitors. Expected rate of overlap (black line) modeled on the first 8 hours of internalization (red arrow for comparison, no inhibitor present), shows good fitting with the remainder of the data ($R^2 = .91$, $\chi^2 = 1.62$, $P > 0.95$).

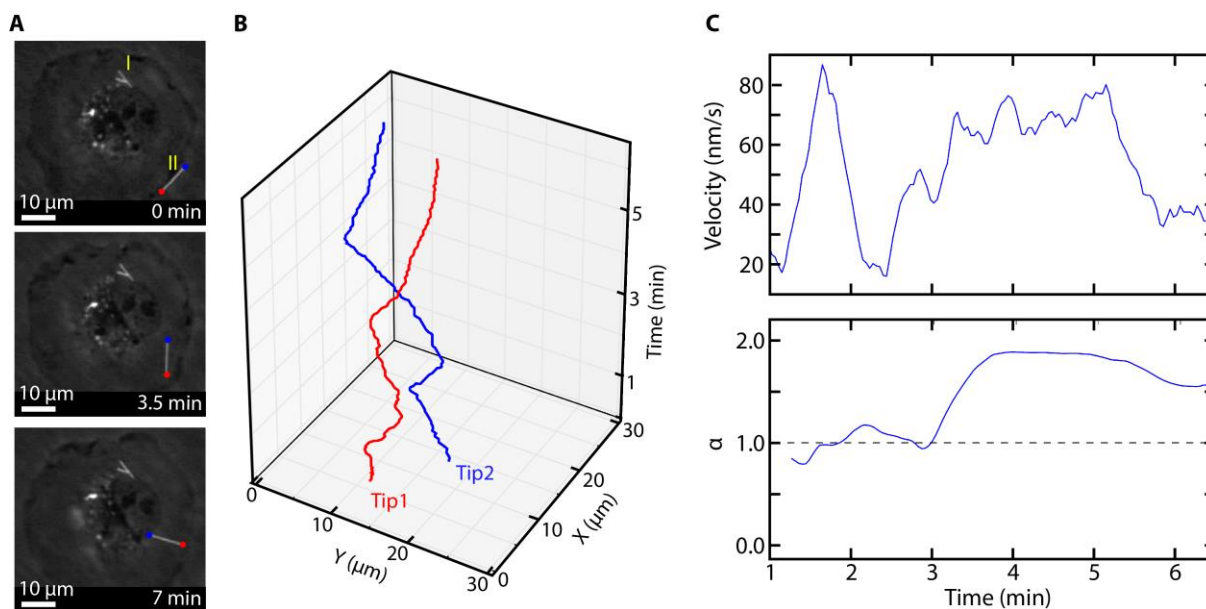


fig. S15. Multiple internalization events. (A) SEPC micrographs of a secondary SiNW (II) being internalized by a HUVEC after it has already internalized another initial group of SiNWs (I) (Scale bar 10 μm). Frames shown at 3.5 min intervals (B) Path of travel for both tips of the secondary SiNW as a function of time. (C) Instantaneous velocity of the SiNW, during internalization, with the corresponding 'diffusivity exponent', α , indicating a similar uptake processes occurs for secondary wires. Diffusivity exponent, α , was obtained over a rolling 60 frame period. All values given for tip 2 (blue).

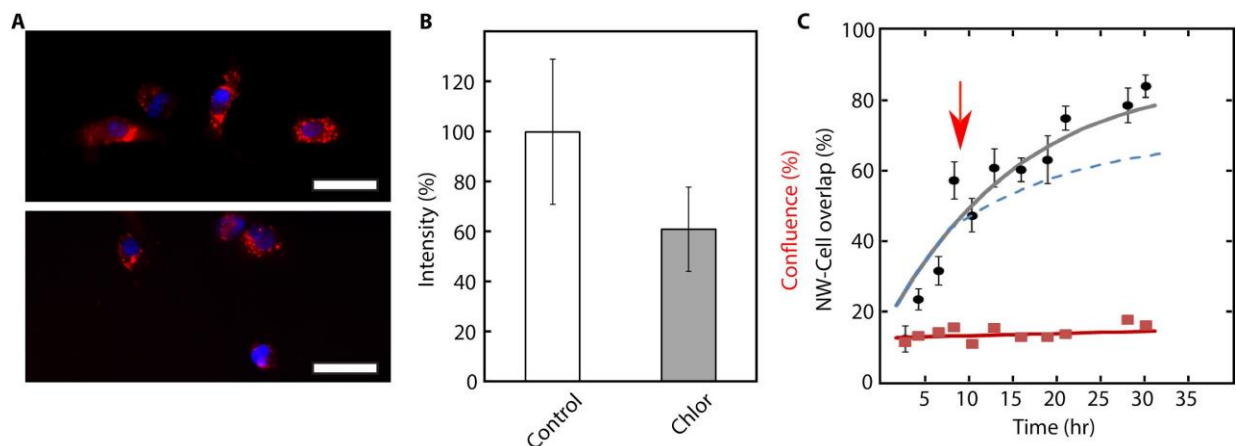


fig. S16. Chlorpromazine-positive control. (A) Example fluorescent staining micrograph after Texas Red conjugated transferrin incubation in a control sample (upper) and chlorpromazine (lower) treated cells (Scale bar 50 μm)(Red-Transferrin) (Blue-DAPI). (B) Relative signal intensity of transferrin per cell treated with 2.5 μg/mL of chlorpromazine (14 hrs) compared to a control sample, showing effective clathrin dependent endocytosis inhibition ($P < 0.01$). (C) Observed SiNW/Cell overlap (black dots) & cell confluence (red dots) as a function of time for chlorpromazine drug studies, with modeled fit (black line). Blue-dashed line gives the expected rate of SiNW internalization if the uptake process was clathrin dependent given the measured blocking levels. Experimentally observed overlap deviates significantly from the projected blocking ($\chi^2(6, N = 6) = 16.9, P < 0.01$), suggesting the observed process was not clathrin dependent.

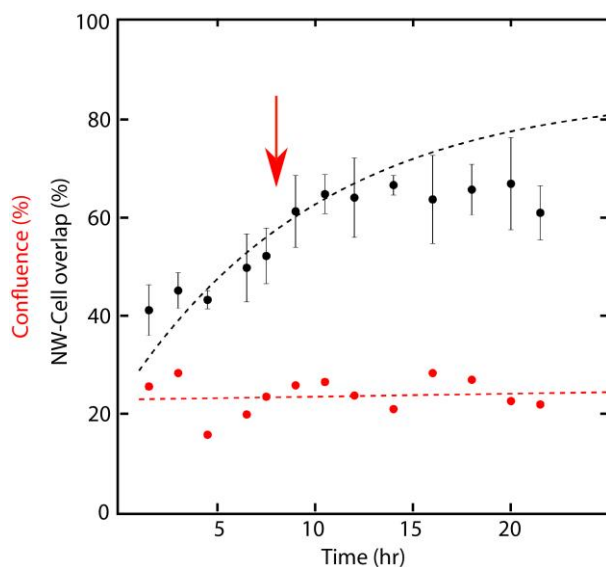


fig. S17. High-concentration A5 study. Observed SiNW/Cell overlap (black dots) & cell confluence (red dots) as a function of time for 16 nM A5 drug studies, with internal control modeled fit (black line). Experimentally observed overlap shows a greater reduction in SiNW uptake than 4 nM A5 concentrations.

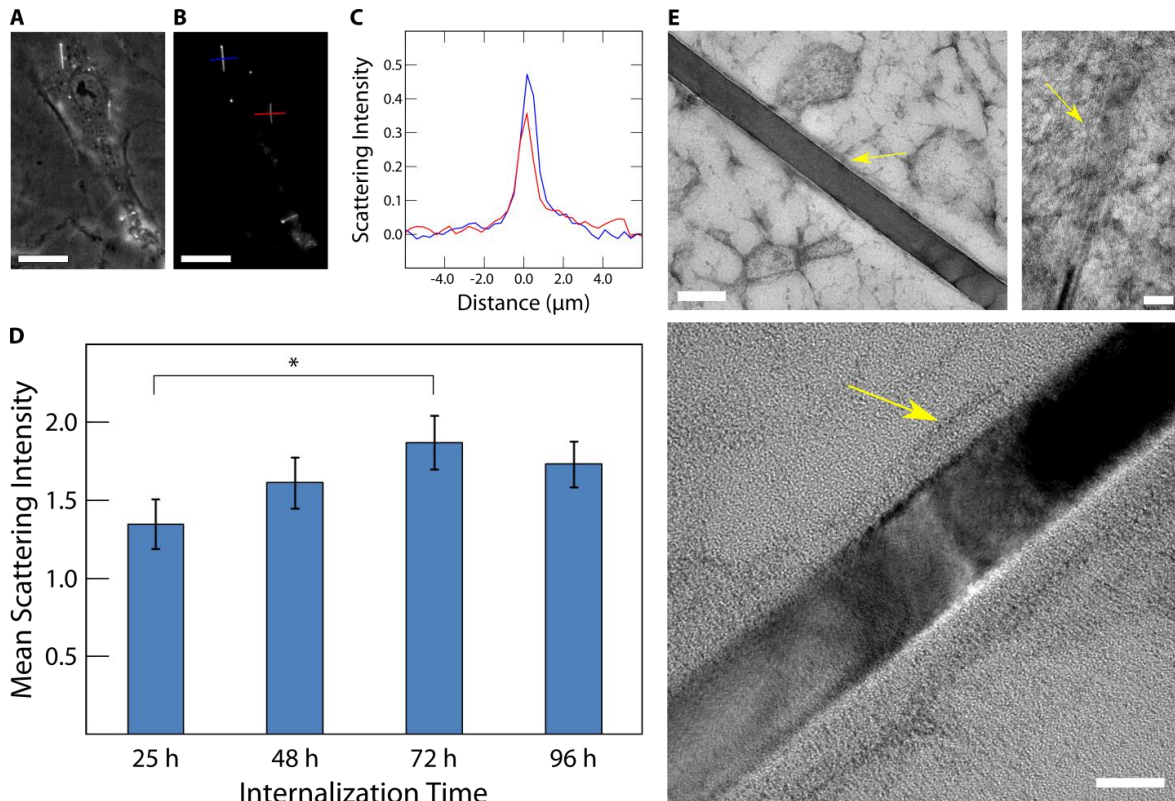


fig. S18. Cytosolic SiNW protein sheath formation. (A) Example SEPC and (B) DF micrographs of SiNWs (mean diameter = 100 nm) incubated with HUVEC for 25 h, with (C) the accompanying line-scans used to determine the SiNWs' maximum scattering intensity, taken over the highlighted regions (blue & red). Scattering intensities given relative to maximum observed scattering. (D) Mean scattering intensity of SiNWs incubated with HUVECs over time (* indicates statistical significance, $P < 0.05$, $N > 30$), normalized by the scattering intensity of a control population of SiNWs incubated in deionized water (DI) over the same time period (37°C , $5\% \text{CO}_2$). DI control population showed no significant change in scattering over the incubation period ($N > 135$). Increase in SiNW scattering likely corresponding to the formation of a protein corona. Error bars given as standard error of the mean. (E) Example TEM micrographs of internalized cytosolic SiNWs surrounded by a thin layer of proteins, or 'protein corona'. Yellow arrows help indicate the location of the protein sheath (Scale bars: top left-200 nm, top right-50 nm, & bottom-25 nm respectively).

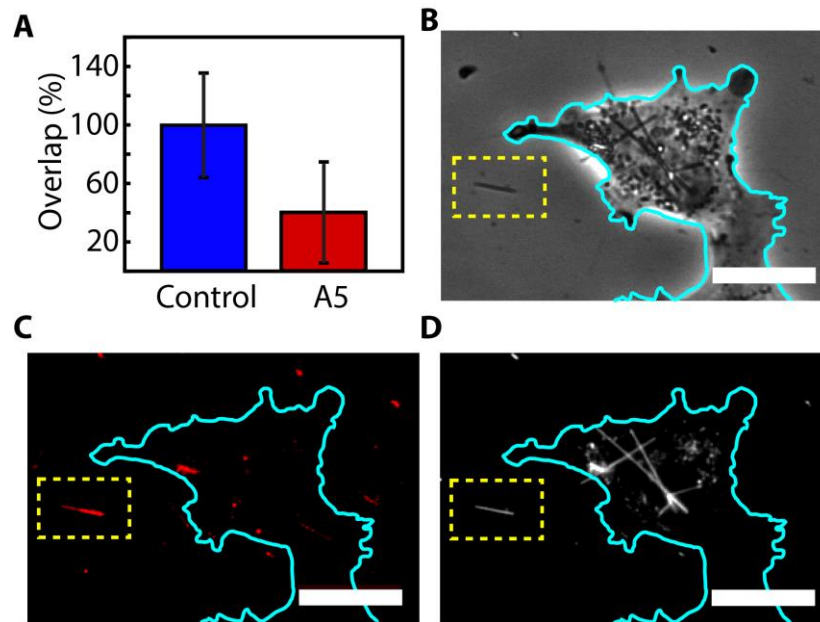


fig. S19. Prestained A5 SiNWs. SiNWs pre-stained with A5-Cy3 were incubated with HUVECs for 24 hrs. (A) NW-Cell overlap of SiNWs retaining their Cy3-A5 coating (red), normalized to the overlap of uncoated SiNWs (blue), indicating a greatly reduced uptake of A5 bound wires ($P < 0.1$). Example micrograph showing the same region in the PC (B), Cy3 (C), and DF channels (D), indicating the SiNW retaining its Cy3-A5 coating is excluded from the cell. DF and Cy3 backgrounds subtracted using a Gaussian spatial filter uniformly applied to each image (SiNW-yellow, Cell Outline-teal) (Scale Bars 25 μm).

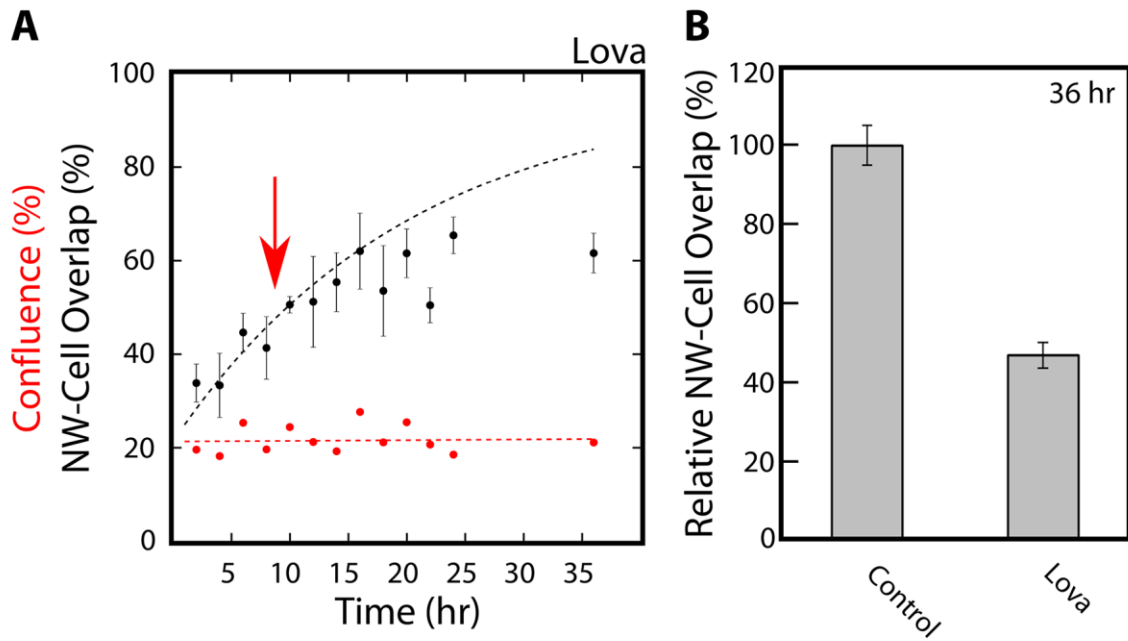


fig. S20. Lovastatin inhibitor study. (A) Observed SiNW/Cell overlap (black dots) & cell confluence (red dots) as a function of time for lovastatin treated cells (10 μm) (drug administered at red arrow), with internal control modeled fit (black line). Error bars given as the standard deviation. (B) Relative increase in SiNW overlap between drug's administration at 8h and 36h, in an external negative control and lovastatin treated cells, showing an ~52% reduction in SiNW internalization. Error bars given as the standard error of measurement.

Supplementary Movies

movie S1. Single-cell SiNW active transport. (A) SEPC micrograph of a SiNW during internalization (Scale bar 15 μ m). (B) MSD 'diffusivity exponent', α , indicating mode of active vs restricted-diffusive transport. Diffusivity exponent, α , was obtained over a rolling 30 frame period. (C) Instantaneous velocity of the SiNW's time (15 frame average). All values given for tip 1 (red). (D) Path of travel for both tips of the SiNW as a function of time (red=upper tip, blue=lower tip).

movie S2. Bidirectional active tug-of-war SiNW transport. Time-lapse SEPC micrograph of a SiNW co-cultured with HASMCs, 3 days after initial incubation, showing large bursts of bidirectional active transport (200x play speed, Scale bar 20 μ m).

movie S3. Macrophage internalization of SiNWs. SEPC micrograph of a mouse derived J774A.1 macrophage internalizing a SiNW during co-culture (60x play speed, Scale bar 15 μ m).

movie S4. SiNW membrane engulfment. SEPC micrograph of a membrane protrusion extending along a single long SiNW during internalization (160x play speed, Scale bar 8 μ m).